

Total electron-loss cross sections and absolute charge-state yields of 20-MeV Fe ions transmitted through gaseous targets

H. Knudsen,* C. D. Moak, C. M. Jones, P. D. Miller, R. O. Sayer, and G. D. Alton
Oak Ridge National Laboratory, Oak Ridge, Tennessee 37830

L. B. Bridwell

Murray State University, Murray, Kentucky 42071

(Received 14 August 1978)

Absolute charge-state yields of 20-MeV Fe ions emerging within a large acceptance angle from a differentially pumped gas cell of length 9.4 cm have been measured using N₂, Ar, Kr, Xe, and SF₆ targets. The gas pressures ranged from 2 to 400 mTorr, thereby including target thicknesses where single events dominate the charge change, as well as target thicknesses where charge-state equilibrium is established. From the low-pressure yields total cross sections, σ_{4q} with $q = 5-15$ were obtained using an improved version of the initial growth method.

I. INTRODUCTION

In recent years the study of the interaction of energetic ions with matter has received appreciable attention. Of particular interest are the processes causing the projectile and the target atoms to change charge. Cross sections for electron capture and loss for light ions have been reported in detail,¹ whereas similar information for heavy ions is rather sparse. As theoretical attempts to calculate such cross sections have proven to be extremely difficult, it is important to obtain extended experimental data, partly because of practical interest, partly to help clarify our understanding of the complicated charge-changing mechanisms.

A comprehensive review by Betz² contains theoretical and experimental results for total cross sections and charge-state distributions. In addition, a number of experiments have been performed to measure differential charge-changing cross sections in order to obtain information on the impact-parameter dependence of the electron capture and loss.³⁻⁶ The yield of charge states emerging from solid and gaseous targets has become important due to the use of stripping techniques in several types of accelerators. As an example, Moak *et al.*⁷ published absolute charge-state yields of 20-MeV I ions emerging from N₂, Ar, Kr, and Xe gas targets.

Here we present measurements of absolute charge-state yields of 20-MeV Fe ions emerging from gaseous targets of N₂, Ar, Kr, Xe, and SF₆. The acceptance angle was large enough so that essentially all particles entering the target were analyzed. The pressure ranged from 2 to 400 mTorr, thereby covering both the low-pressure region where single events dominate the

charge change as well as the high-pressure region where equilibrium conditions are met. From the low-pressure yields, we have calculated the total cross sections for loss of one electron and loss of multiple electrons in a single event, and the cross sections for loss of the initial charge state, which in this experiment was +4. The method used for obtaining the cross sections was an improved version of the "initial growth" technique.

II. EXPERIMENTAL PROCEDURE

The experimental apparatus was the same as that used for measurements of absolute charge-state yields of 20-MeV I ions reported in Ref. 7. The experimental arrangement was shown in Fig. 1 of that paper, and the apparatus and experimental procedure were described in detail. For the present experiment a beam of 20-MeV Fe⁴⁺ ions was obtained from the Oak Ridge EN tandem. The absolute intensity of the incident beam was measured relative to a monitor, as described in Ref. 7. For this experiment, the ratio of incident particles per monitor detector count was constant within $\pm 3\%$ throughout the experiment. At pressures below 0.10 Torr of all gases, the sum over charge states of the yields per incident particle was 1.0 within the statistical error indicating that scattering of the beam both before and after the gas cell was negligible. The effect of scattering on the absolute yields at pressures ≥ 0.10 Torr will be discussed in Sec. V.

The detection system consisted of a carefully aligned magnetic quadrupole lens which was used to focus ions of a selected charge state into an electrostatic analyzer followed by a position-sensitive detector. This detector was movable, and when calibrating the monitor system it was fully

withdrawn so as to expose the end detector. During charge-state yield measurements two other positions were used. With the detector positioned so as to intercept the beam axis, charges 0 to +11 could be measured. With the detector partly withdrawn, charges +11 to +15 could be measured. Because of power supply limitations, the quadrupole lens could not focus charge states below +7. However, at low gas pressures, the scattering in the cell was so small, and the angular distributions are so peaked forward that all low-charge-state peaks were well resolved and totally collected, and therefore, these yields could be measured accurately with the lens set to focus charge +7. The spectra were very similar to those shown in Fig. 2 of Ref. 7. Count rates in the position-sensitive detector were held to ~1000 counts/sec so as to minimize spectra distortion and dead time.

In order to obtain absolute charge-state yields, the number of particles of a selected and well-resolved charge state per monitor count was measured. The product of this number and the ratio of monitor counts to end detector counts then gave the desired result.

For most of the target gases and gas pressures used in this experiment we found no difference between the absolute yields obtained using 4- and 8-mrad acceptance angles. In the case of Xe gas, which contains the heaviest of the target atoms used here, we observed ~10% lower yields using the 4-mrad aperture for the highest charge states (+13, +14, and +15). However, as this difference is so small, we feel confident that the 8-mrad acceptance angle is sufficiently large to accept virtually all particles emerging from the gas cell.

The pressure in the beam line was kept below 3×10^{-6} Torr except in the immediate neighborhood of the gas cell at the highest cell pressures. This assured a rather pure beam of charge state +4 ions. However, with no target gas in the cell, we found small traces of +5, +6, +7, and higher charge state ions of 2.2%, 1.0%, 0.8%, and lower percentages, respectively.

III. DATA TREATMENT

When a beam of ions, originally of charge state +4, is passed through a gas cell containing a target gas pressure ϕ , then, in the case that ϕ is small and under ideal experimental conditions, the absolute yield of ions emerging with charge state + q ($q \neq 4$) will be given by

$$Y_q = \sigma_{4q}\phi + A_q\phi^2 + B_q\phi^3 + \dots \quad (1)$$

Here σ_{4q} is the total cross section for going from charge state +4 to charge state + q . The first

term stems from single events and is proportional to the target pressure. The following terms are due to double, triple, etc. events. For example, A_q is given by

$$A_q = \frac{1}{2} \left[\sum_{\substack{i \neq 4 \\ i \neq q}} \sigma_{4i}\sigma_{iq} - \sigma_{4q} \left(\sum_{j \neq 4} \sigma_{4j} + \sum_{k \neq q} \sigma_{qk} \right) \right] \quad (2)$$

Our data treatment is complicated by the fact that we observe a yield $Y_q(P=0)$, where P is the pressure *measured* in the gas cell, that is different from zero for $q \neq 4$. This is caused by interaction of the primary beam with the residual gas in the beam line. We correct for the effect of the residual gas by assuming that it gives the same yield as an equivalent amount P_0 of the target gas situated in the gas cell. Then the yield observed at the *measured* pressure P is actually $Y_q(\phi = P + P_0)$. From Eq. (1) we find that

$$\frac{Y_q(P + P_0) - Y_q(P_0)}{P} = [\sigma_{4q} + 2A_qP_0] + A_qP + \dots, \quad (3)$$

$$\frac{Y_q(P + P_0) - Y_q(P_0)}{P} = \sigma_{4q} + A_q[P + 2P_0] + \dots \quad (4)$$

Therefore, when plotting $[Y_q(P + P_0) - Y_q(P_0)]/P$ as a function of P , we obtain a constant if only single events play a role, and a straight line with slope A_q if double events are important, too. In both cases, the left-hand side of Eq. (3) extrapolates to

$$\sigma'_{4q} = \sigma_{4q} + 2A_qP_0 \quad (5)$$

for $P = 0$.

Using σ'_{4q} as a first estimate of σ_{4q} we then find the equivalent residual gas pressure P_0 from

$$P_0 = Y_q(P_0)/\sigma'_{4q} \quad (6)$$

Since P_0 is derived anew for each value of q , it is the pressure of target gas which is equivalent to the residual gas for that charge state. Therefore no assumption is made about similarity of cross sections of the target and residual gases.

From Eq. (4) it is seen that a plot of the left-hand quantity of Eq. (3) as a function of $P + 2P_0$ will extrapolate to σ_{4q} for $P + 2P_0 = 0$. Such a plot is shown in Fig. 1 for ions of charge state +6 emerging from a Kr target. It is observed that the experimental points fall on a straight line for pressures below ~15 mTorr, indicating that for these small pressures triple and higher-order events are negligible. From the extrapolated value σ'_{46} and the observed yield $Y_6(P_0)$, a value of $P_0 = 0.5$ mTorr was obtained using Eq. (6). This

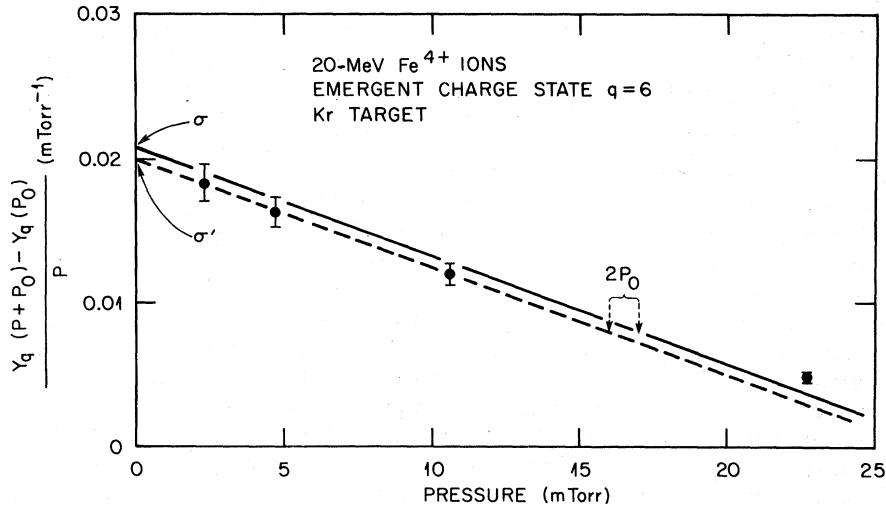


FIG. 1. Example of the extrapolation that was performed for each target gas and each charge state to obtain the preliminary value of the cross section σ' and then the final value σ .

value was then used to find σ_{46} .

In all cases, P_0 was found to be small, and the correction $\sigma - \sigma'$ due to P_0 was correspondingly small. Therefore, no further iterations were necessary. For all target gases, and for the lowest charge states, P_0 was found to be close to 0.5 mTorr. However, P_0 varies with q in such a way as to decrease with increasing q . This may be understood by noting that high charge states are created mainly in collisions with small impact parameters giving large deflections of the ions. Therefore, in the long beam line preceding the gas cell, some of the ions which reach high charge states by interacting with the residual gas are scattered away from the beam, resulting in relatively lower $Y_q(P_0)$ and consequently lower P_0 values than those found at small q .

For the majority of cases investigated in this work, the experimental values of $P^{-1}[Y_q(P+P_0) - Y_q(P_0)]$ were found to fall on a straight line for the lowest target gas pressures (~ 2 , ~ 5 , and ~ 10 mTorr). This indicates that triple or multiple events are negligible at those pressures and consequently that the values of σ_{4q} were obtained in a self-consistent way. However, for SF_6 target gas and $q < 12$ and for all charge states for Xe gas the three low-pressure points did not fall on a straight line. In those cases where the deviation from a straight line was small, we extrapolated to $P + 2P_0 = 0$ using only the points obtained at ~ 2 and ~ 5 mTorr. This introduced some uncertainty into the data treatment and this has been indicated by placing parentheses around the corresponding cross-section points in the following figures. In cases where the

deviation from a straight line was significant, no cross sections were derived. For N_2 gas, the experimental uncertainty of the cross section values σ_{4q} , $q > 4$, was found to be $\sim \pm 6\%$ for $q < 12$ and $\sim \pm 10\%$ for $q \geq 12$. For Ar, Kr, and Xe gas, it is $\sim \pm 7\%$ for all charge states, and for SF_6 it is $\sim \pm 8\%$ for the charge states $11 \leq q \leq 14$.

The method for obtaining electron-loss sections used here is an improved version of the simple initial growth method. The drawbacks of the simple method have been discussed by Datz *et al.*⁸ Our improved method eliminated the problems mentioned there. A similar data treatment has been used previously by Heinemeier *et al.*⁹

The number of ions retaining charge-state 4 when passing through the gas cell decreases with increasing target pressure. The cross section for loss of charge state 4, $\sigma_{4,\text{loss}}$, is defined as

$$\sigma_{4,\text{loss}} = \sum_{q \neq 4} \sigma_{4q}. \quad (7)$$

It was obtained from the measured absolute yield of 4+ ions in the following way: From the values of P_0 obtained for $q > 4$ we extrapolate to $q = 4$ to find the proper P_0 value. Then, when plotting Y_4 as a function of $P + P_0$ we find that the data points fall on a straight line on a semilogarithmic plot according to the equation

$$Y_4 = \exp[-\sigma_{4,\text{loss}}(P + P_0)]. \quad (8)$$

From the slope of the straight line, $\sigma_{4,\text{loss}}$ can be found. That the method is self-consistent is proven by the fact that the value of P_0 found from

$$Y_4(P_0) = \exp(-\sigma_{4,\text{loss}} P_0) \quad (9)$$

coincides with the value extrapolated from the higher charge states. The experimental uncertainty associated with our measured values of $\sigma_{4,\text{loss}}$ is $\sim \pm 6\%$ for N_2 , Ar, Kr, and Xe, whereas it is $\pm 15\%$ for SF_6 .

Although we did not measure the yield of particles with $q < 4$, the capture cross section σ_{43} can, in principle, be found from the experimental values of $\sigma_{4,\text{loss}}$ and σ_{4q} , $q > 4$, through

$$\sigma_{43} \approx \sum_{q < 4} \sigma_{4q} = \sigma_{4,\text{loss}} - \sum_{q > 4} \sigma_{4q}, \quad (10)$$

since the cross section for double capture, σ_{42} , is probably very much smaller than σ_{43} . However, σ_{43} , obtained in this way as a difference between two large numbers, has a substantial uncertainty. Therefore, only an upper limit of its magnitude will be given here: For N_2 , Ar, Kr, and Xe, σ_{43} was found to be smaller than $\sim 20\%$ of the corresponding value of $\sigma_{4,\text{loss}}$.

In Sec. IV we present the cross sections for electron loss and $\sigma_{4,\text{loss}}$. They were found using the procedure for data treatment discussed above as cross sections *per molecule* in units of reciprocal pressure (mTorr^{-1}). However, they will be presented here as cross sections *per atom* in units of cm^2 . To convert the experimental values we divided the cross sections for N_2 by 2 and those for SF_6 by 7, and used the formula

$$X(\text{molecules}/\text{cm}^2) = 3.30 \times 10^{13} P(\text{mTorr}) L(\text{cm}), \quad (11)$$

where X is the target thickness and L its effective length. The temperature was 20°C .

IV. CHARGE-CHANGE CROSS SECTIONS

The cross sections per target atom for loss of one electron measured in this work for 20-MeV Fe^{4+} ions are shown in Fig. 2. Their magnitude is of the order of 1 \AA^2 , indicating that loss of one electron can occur in even very weak collisions in which the distances of closest approach are around $0.5\text{--}1 \text{ \AA}$. This corresponds to the target atomic nucleus penetrating only the outermost parts of the Fe-ion electron distribution. Similar results have been found previously, for example, by Scott *et al.*,⁶ who observed the maximum of the +5 charge-state fraction for 20-MeV Cl^{4+} ions transmitted through nitrogen gas to appear at a scattering angle corresponding to an impact parameter of 0.3 \AA .

As can be seen in Fig. 2, the single-electron-

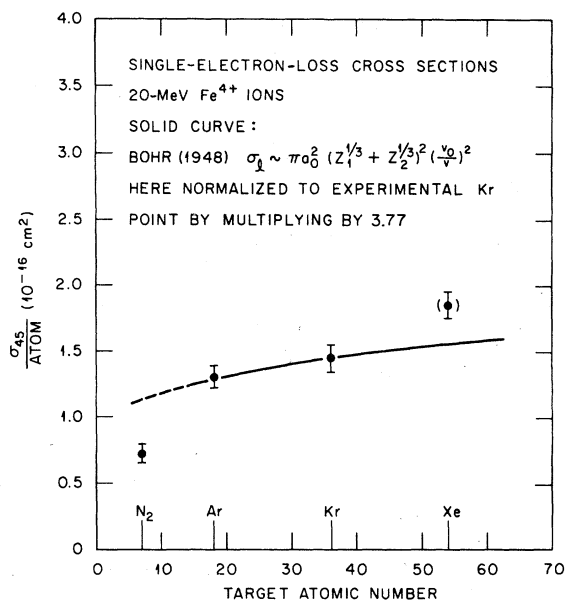


FIG. 2. Total single-electron-loss cross sections obtained in this work, compared to the target atomic-number dependence of the simple Bohr estimate. The significance of data points in parentheses is discussed in the text.

loss cross sections measured on noble-gas targets increase slowly with increasing target atomic number. This dependence was predicted by Bohr in his comprehensive 1948 paper.¹⁰ He assumed that for heavy ions colliding with heavy atoms, loss is likely to take place whenever the ion penetrates a region of the target atom containing electrons of orbital velocities comparable to the ion velocity v . Considering the radial extension of such electrons, he arrived at the expression

$$\sigma_1 \sim \pi a_0^2 (Z_1^{1/3} + Z_2^{1/3})^2 (v_0/v)^2, \quad (12)$$

where σ_1 is the single-electron-loss cross section, a_0 the Bohr radius, v_0 the Bohr velocity, and Z_1 and Z_2 the atomic numbers of projectile and target atom, respectively. In Fig. 2 Bohr's result is shown, normalized to our experimental Kr point. It reproduces fairly well the target atomic-number dependence of our Ar, Kr, and Xe results, while the N_2 point is lower than expected from Eq. (12). The largest part of the N_2 difference is probably due to the fact that the Bohr estimate is valid only for large Z_2 . For small Z_2 the cross section should decrease more rapidly with decreasing target atomic number than expected from Eq. (12). However, it should be noted, that the nitrogen

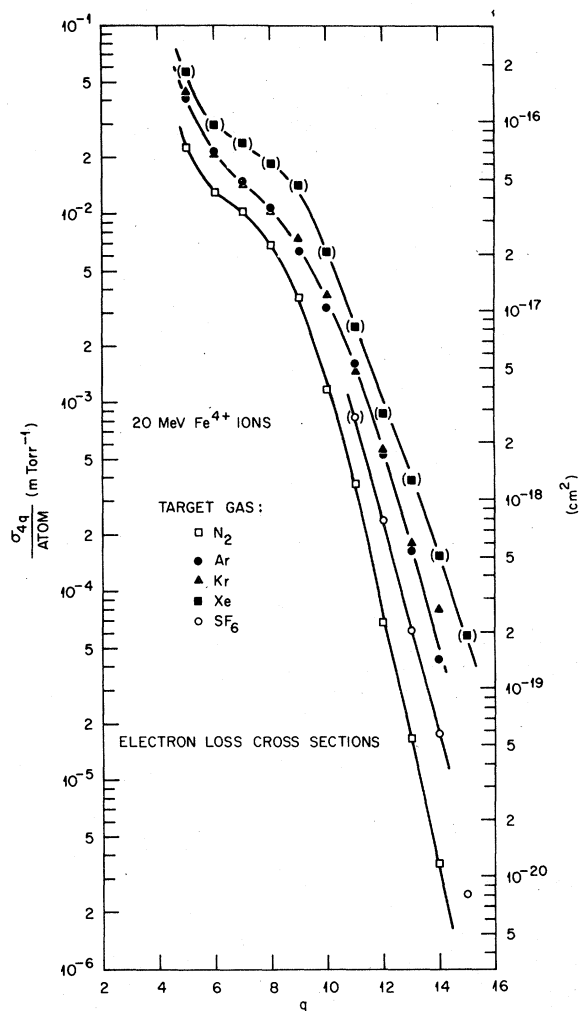


FIG. 3. Total single- and multiple-electron-loss cross sections, plotted as function of the final charge state q . The gas cell length was 9.4 cm. The curves are drawn to guide the eye. The significance of data points in parentheses is discussed in the text.

target gas is molecular and does not consist of isolated atoms. Therefore, the experimental N_2 result might also be influenced by the molecular structure. Recently it was found experimentally that molecular spatial correlation between target atoms causes a decrease in small-angle single¹¹ and multiple^{12,13} scattering as compared to the case for a dissociated target gas. These effects were investigated theoretically by Sigmund.¹⁴ Evidence for effects stemming from molecular structure in charge-exchange phenomena has been found, for example, by Wittkower and Betz,¹⁵ who showed that cross sections $\sigma_{5,q}$ for 12-MeV I ions

transmitted through C_3H_6O were significantly smaller than any possible addition of cross sections for its components. Betz² discussed the nonadditivity of molecular charge-exchange cross sections in his review paper.

The measured total cross sections per target atom for loss of 1 to 11 electrons in a single collision for 20-MeV Fe^{4+} ions transmitted through gases of N_2 , SF_6 , Ar, Kr, and Xe are shown in Fig. 3 as a function of the final charge state, q . For each of the target gases, the data show the same trend as a function of q : There is an overall rather steep decrease for increasing q , interrupted by a weaker decrease between $q=6$ and $q=8$. For the highest q values, the cross sections follow a nearly exponential decrease with q . Defining

$$r_q = \sigma(4, q+1)/\sigma(4, q), \quad (13)$$

we find that r_5 (that is the ratio between the double- and the single-electron-loss cross section) is ~ 0.5 for all the target gases. Then, for example, for Kr gas target, $r_6 \approx r_7 \approx r_8 \approx 0.7$, followed by an abrupt decrease to a value of $r_q \approx 0.4$ for $q > 8$. Comparing the results for the different gases, it is observed that the cross sections are smaller, and the decrease at high- q values is more pronounced, the lighter the target atoms.

The data of Fig. 3 may be compared to the results of Moak *et al.*¹⁶ They measured electron-loss cross sections for 110-MeV I^{12+} in H_2 , He, and Ar and for 162-MeV I^{17+} in O_2 . The 162-MeV results show a dependence on q similar to that observed in this work: the cross sections decrease steeply with increasing q , interrupted by

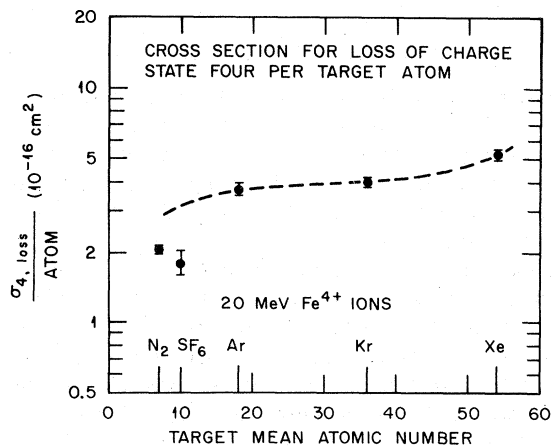


FIG. 4. Cross sections for loss of charge state 4. The dashed curve is drawn to show a possible extrapolation of the noble-gas data towards lower atomic number targets.

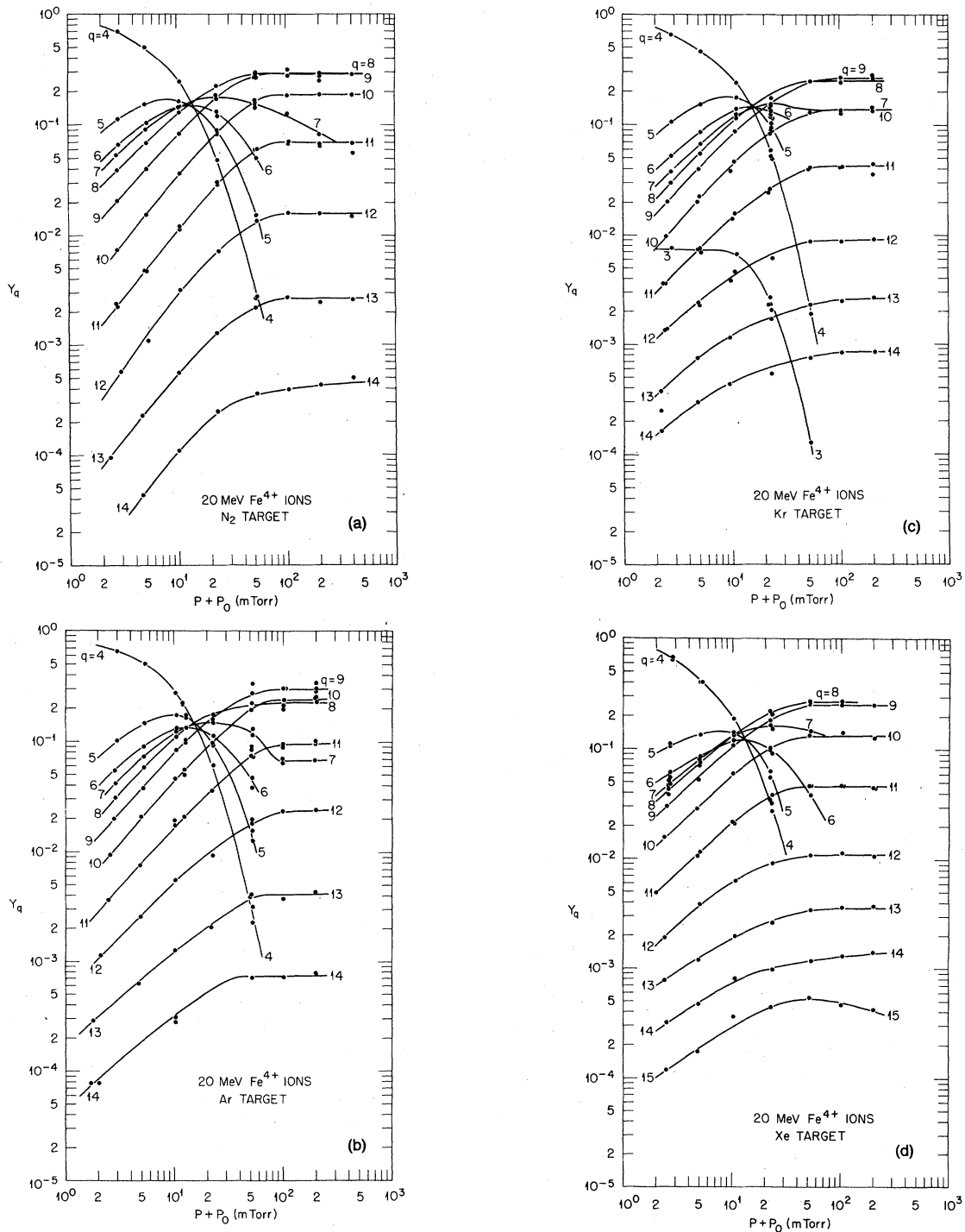


FIG. 5. (a) Absolute yield of 20-MeV Fe ions emerging from a 9.4 cm long gas cell within an acceptance angle of 8 mrad, plotted for each charge state as a function of N_2 target gas pressure. (b) Absolute yield of 20-MeV Fe ions emerging from a 9.4 cm long gas cell within an acceptance angle of 8 mrad, plotted for each charge state as a function of Ar target gas pressure. (c) Absolute yield of 20-MeV Fe ions emerging from a 9.4 cm long gas cell within an acceptance angle of 8 mrad, plotted for each charge state as a function of Kr target gas pressure. (d) Absolute yield of 20-MeV Fe ions emerging from a 9.4 cm long gas cell within an acceptance angle of 8 mrad, plotted for each charge state as a function of Xe target gas pressure. (e) Absolute yield of 20-MeV Fe ions emerging from a 9.4 cm long gas cell within an acceptance angle of 8 mrad, plotted for each charge state as a function of SF_6 target gas pressure.

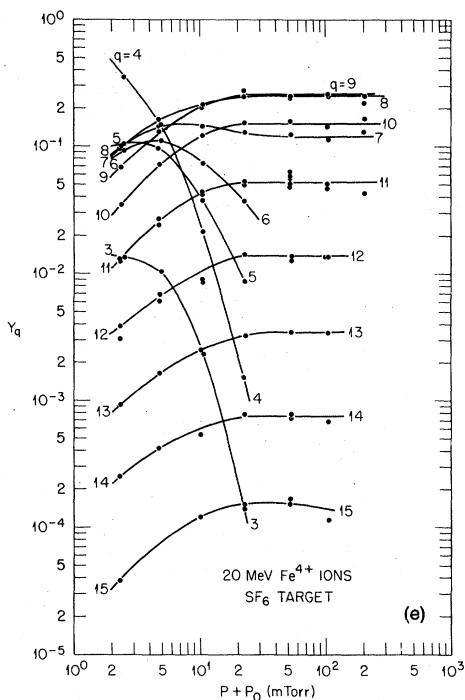


FIG. 5. (Continued)

a relatively slow decline in the region $q = 18$ to $q = 25$. For their 110-MeV measurements, the cross sections are very much smaller for H_2 and He and they decrease more rapidly with q than the data obtained on Ar atoms. Similar results have been found by Betz *et al.*¹⁷ and by Betz and Wittkower¹⁸ for 15-MeV I ions passing through H_2 , He, and O_2 gases and by Scott *et al.*⁶ for 20-MeV Cl and I ions incident on N_2 , Ar, and Xe.

Betz² suggested a qualitative explanation of the observed effects. He distinguishes between two basically different processes for electron loss. In the first, individual electrons are lost via a direct interaction with the target atoms. Therefore the loss of an individual electron should occur independently of the presence of other electrons and this mechanism should apply primarily to the removal of electrons from the outer shells of the ion (low- q). In the second process, the ion and the target atoms form a pseudomolecule during the collision and, through promotion and level crossing, the ion emerges after the encounter in a highly excited and/or ionized state. The following deexcitation may cause Auger processes which lead to the removal of more electrons. This mechanism should account for the many-electron-loss cross sections (high- q) and should be more important when more electrons are available in

the pseudomolecule. Finally Betz speculates that both mechanisms might be effective in the region of intermediate- q values, thereby causing the relatively weak decrease of the cross sections observed there. This model explains qualitatively both the q dependence of our observed cross sections and the dependence on target atomic number. Especially it accounts for the increasingly steep decrease of the cross sections at high- q values going from the heavy to the light target atoms as being due to the fact that the light atoms are not as effective in forming low-lying pseudomolecular states as are the heavy target atoms.

It should be noted that the model of Betz does not explicitly involve shell effects in the explanation of the less steep part of the cross-section curves. Therefore it does not readily explain the fact that the abrupt change in the slope occurs at closed shells or subshells of the ion. In this work, we find the "shoulder" to appear at $q = 8$ for Fe ions where the $3p$ subshell is closed, while Moak *et al.*¹⁶ found it at $q = 25$, where the M shell of the I ions investigated in their work is closed. These shell effects point to a mechanism more directly related to the ionization potential of the highly ionized ions.

Multiple electron loss is a highly probable outcome of heavy-ion-heavy-atom collisions. As mentioned above, we find the cross section for double electron loss to be only ~50% smaller than the single-loss cross section. Furthermore, we find the total cross section for loss of more than one electron in one collision

$$\sigma_{4, q>5} = \sum_{q>5} \sigma_{4q} \quad (14)$$

to be equal to ~1.5 times the single-loss cross section for the target gases where Eq. (14) can be calculated, that is, for N_2 , Ar, Kr, and Xe. A similar result was reported by Moak *et al.*¹⁶ for 110-MeV I^{12+} ions in Ar and by Datz *et al.*⁸ for 13.9- and 25-MeV Br ions in Ar.

The experimental values of the total cross sections per target atom for loss of charge state 4, $\sigma_{4, \text{loss}}$, are shown in Fig. 4, plotted versus the target mean atomic number. As is the case for σ_{45} , $\sigma_{4, \text{loss}}$ increases slowly with increasing atomic number for the noble-gas targets. And as in Fig. 3, the cross sections obtained on the low Z_2 molecular targets seem to be relatively too small as compared with the trend of the other data. This may again partly be attributed to effects stemming from the spatial correlation between the molecular atoms. This idea is consistent with the fact that the SF_6 cross section is smaller than that which would have been estimated from the other data

in Fig. 4 since SF₆ is a larger molecule containing more atoms than the other target gases.

V. ABSOLUTE CHARGE-STATE YIELDS

Our measurements of absolute charge-state yields were performed both at the low pressures important for extraction of charge-change cross sections and at gas cell pressures where charge-state equilibrium is established. Such yields measured across a broad range of pressures are, besides being of basic interest, important to the design and operation of the gas strippers of large tandem accelerators.

In Figs. 5(a)–5(e) are shown the experimental, absolute charge-state yields of 20-MeV Fe⁴⁺ ions transmitted through N₂, Ar, Kr, Xe, and SF₆ target gases, respectively. These yields were, as mentioned above, obtained within an 8-mrad acceptance angle that included virtually all particles emerging from the gas cell. However, when adding the yields Y_q for each gas, we found that at the highest target gas pressures, the sum was smaller than unity. This effect was attributed to a small broadening of the beam in the gas cell due to scattering, causing a larger image area of the focused charge-state beam at the ~4 mm wide position-sensitive detector, and thus incomplete collection of the ions. At high pressures, the broadening of the image area is expected to be approximately the same for all charge states, and therefore all the yields, obtained at each of the high pressures where this effect was seen, were corrected by the same factor so as to make the sum of the yields equal to unity. This correction was negligible for target pressures below 50 mTorr and amounted at 200-mTorr pressure to 5% for N₂, 25% for Ar, 30% for Kr, and

40% for Xe and SF₆.

From Figs. 5(a)–5(e) information about the maximum obtainable yields for each charge state and target gas may be found, together with the corresponding optimum pressure. The results can be compared to similar data measured by Moak *et al.*⁷ for 20-MeV I⁵⁺ ions transmitted through N₂, Ar, Kr, and Xe stripper gases.

Further, we can find the most probable charge of all ions emerging from the gas cell at equilibrium pressure. For the gases used here it is ~8.5. From the review paper by Betz² (Fig. 5.11) one finds correspondingly a value of 7.8, while a value of 8.1 is obtained from the work of Sayer.¹⁹ The difference between these semiempirical results and our experimental value may be attributed to the so-called density effect: If two target gas cells contain the same target thickness (in molecules/cm²) but are of different lengths with corresponding different densities, ions passing through the shorter cell will have, on the average, less time for deexcitation between collisions and thereby may emerge with higher average charge than those which passed through the long gas cell. For example, Moak *et al.*⁷ saw a difference in the most probable charge of one between charge-state distributions for 20-MeV I ions transmitted through gas cells of lengths 2 and 9.4 cm, respectively.

ACKNOWLEDGMENTS

The authors wish to thank E. G. Richardson for assistance in running the accelerator and Dr. P. Hvelplund for valuable discussions. This research was sponsored by the Division of Physical Research, U. S. Department of Energy, under Contract No. W-7405-eng-26 with the Union Carbide Corporation.

*Permanent address: Institute of Physics, University of Aarhus, DK-8000, Aarhus C, Denmark.

¹V. S. Nikolaev, *Usp. Fiz. Nauk* **85**, 679 (1965); *Sov. Phys. Usp.* **8**, 269 (1965).

²H. D. Betz, *Rev. Mod. Phys.* **44**, 465 (1972).

³D. Hahn, *Winkelstreuung von Ne and Ar Ionen in gas targets*. Inaugural Dissertation (Freien Universität Berlin, 1976) (unpublished).

⁴Q. C. Kessel, *Phys. Rev. A* **2**, 1881 (1970).

⁵R. A. Spicuzza and Q. C. Kessel, *Phys. Rev. A* **14**, 630 (1976).

⁶H. A. Scott, L. B. Bridwell, C. D. Moak, G. D. Alton, C. M. Jones, P. D. Miller, R. O. Sayer, Q. C. Kessel, and A. Antar, *Phys. Rev. A* **18**, 2459 (1978).

⁷C. D. Moak, L. B. Bridwell, H. A. Scott, G. D. Alton,

C. M. Jones, P. D. Miller, R. O. Sayer, Q. C. Kessel, and A. Antar, *Nucl. Instrum. Method*, **150**, 529 (1978).

⁸S. Datz, H. O. Lutz, L. B. Bridwell, C. D. Moak, H. D. Betz, and L. D. Ellsworth, *Phys. Rev. A* **2**, 430 (1970).

⁹J. Heinemeier, P. Hvelplund, and F. R. Simpson, *J. Phys. B* **9**, 2669 (1976).

¹⁰N. Bohr, *K. Dan. Vidensk. Selsk. Mat. Fys. Medd.* **18**, No. 8 (1948).

¹¹P. Loftager (private communication).

¹²G. Sidenius, N. Andersen, P. Sigmund, F. Besenbacher, J. Heinemeier, P. Hvelplund, and H. Knudsen, *Nucl. Instrum. Methods* **134**, 597 (1976).

¹³F. Besenbacher, J. Heinemeier, P. Hvelplund, and H. Knudsen, (unpublished).

¹⁴P. Sigmund, *K. Dan. Vidensk. Selsk. Mat. Fys. Medd.*

- 39, No. 11 (1977).
- ¹⁵A. B. Wittkower and H. D. Betz, *J. Phys. B* 4, 1173 (1971).
- ¹⁶C. D. Moak, H. O. Lutz, L. B. Bridwell, L. C. Northcliffe, and S. Datz, *Phys. Rev.* 176, 427 (1968).
- ¹⁷H. D. Betz, G. Ryding, and A. B. Wittkower, *Phys. Rev. A* 3, 197 (1971).
- ¹⁸H. D. Betz and A. B. Wittkower, *Phys. Rev. A* 6, 1485 (1972).
- ¹⁹R. O. Sayer, *Rev. Phys. Appl.* 12, 1543 (1977).